8A.2 Mobile Mesonet Observations of the Rear-Flank Downdraft Evolution Associated with a Violent Tornado Near Bowdle, SD on 22 May 2010

Catherine Finley[*1], Bruce Lee[1], Christopher Karstens[2], Matthew Grzych and Tim Samaras[3]

[1]WindLogics, Grand Rapids, MN

[2]Iowa Sate University, Ames, IA

[3]National Technical Systems, Littleton, CO

1. INTRODUCTION

TWISTEX 2010 (**T**actical **W**eather **I**nstrumented **S**ampling in/near **T**ornadoes **Ex**periment) was a field experiment designed to collect near-surface data in and near tornadoes. One of the project objectives was to document the kinematic and thermodynamic environment in the vicinity of the rear-flank downdraft (RFD) and rear-flank downdraft gust front (RFDGF), and to try to determine the RFD/RFDGF's contribution to tornadogenesis and tornado maintenance.

On 22 May 2010, four TWISTEX mobile mesonet stations intercepted a tornadic supercell southwest of Lowry, SD. Teams followed the storm east over a three hour period as the storm went through several mesocyclone cycles, some tornadic, others nontornadic. The mesonet sampled the time evolution of several RFDs, including an RFD associated with an EF-4 tornado near Bowdle, SD. Several RFD surges that were associated with tornadogenesis, tornado intensification, and dissipation were also sampled. The evolution of the RFDs will be discussed, with a focus on the thermodynamic and kinematic characteristics of the RFD surges.

2. STORM EVOLUTION AND DATA COLLECTION

Data was collected with an array of four mobile mesonet stations similar in design to those described by Straka et al. (1996) using updated versions of equipment wherever possible. Atmospheric variables were sampled every 1 second, and the data was quality controlled using criteria similar to Markowski et al. (2002) and Grzych et al. (2007), and bias corrected prior to analysis.

Each variable sampled was then averaged over a 5 second period to remove very small timescale fluctuations. Unless otherwise noted, all data plots shown are averaged data. In addition to the measured atmospheric quantities, several derived variables were calculated including CAPE, CIN, θ_v and θ_e, and departures of the potential temperature variables from their prestorm environment values (θ_v' and θ_e'). Environmental conditions were calculated using two 5-minute periods of mesonet observations taken in storm inflow prior to the initial storm intercept (~2230 UTC), and following the final intercept (~ 0045 UTC).

Time–space conversion was applied in a manner similar to Markowski et al. (2002) to try to gain some understanding of the two-dimensional structure in the RFD region of the storm. For time-space conversion, one must assume the storm is in 'steady-state' for some specified period of time. The position of the mesonets can then be plotted relative to the storm creating a quasi-2D view of the atmosphere. Since radar data was available at ~ 5 minute intervals, time-space conversion was done over a 5-6 minute period with full appreciation that it was highly unlikely that the storm was in 'steady-state' for that period. Thus, as one views data points further from the center time of the time-space conversion, the analyzed fields become less certain. Storm motion for the time-space conversion was calculated from the average motion of the mesocyclone (as identified in the KABR 0.5 degree elevation scans of the velocity fields) between 2240 – 2318 UTC, the calculated motion of the large tornado (which encompassed much of the low-level mesocyclone) from 2322 – 2339 UTC, and the KABR mesocyclone positions from 2339 – 2348 UTC.

The storm of interest in this study developed near a trough - warm front intersection in north-central South Dakota. A sounding analysis using a RUC analysis vertical profile just east of Bowdle at 2300 UTC modified with the mesonet average inflow observations indicated ~ 4800 J kg^{-1} of CAPE with modest CIN (-51 J kg^{-1}) at this time. The storm-relative 0-3 km helicity, calculated using actual storm motion, was 306 m^2 s^{-2}, most of which was in the 0-1 km layer (240 m^2 s^{-2}). The mesonet teams intercepted the storm at approximately 2230 UTC 5 miles southwest of Lowry soon after the storm began to exhibit supercell characteristics. Over the next several hours the storm moved northeast producing several tornadoes that ranged from EF0 – EF4 intensity.

[*] *Corresponding author address*: Dr. Cathy Finley, Windlogics, Itasca Technology Center, 201 NW 4th Street, Grand Rapids, MN 55744
email: cfinley@windlogics.com

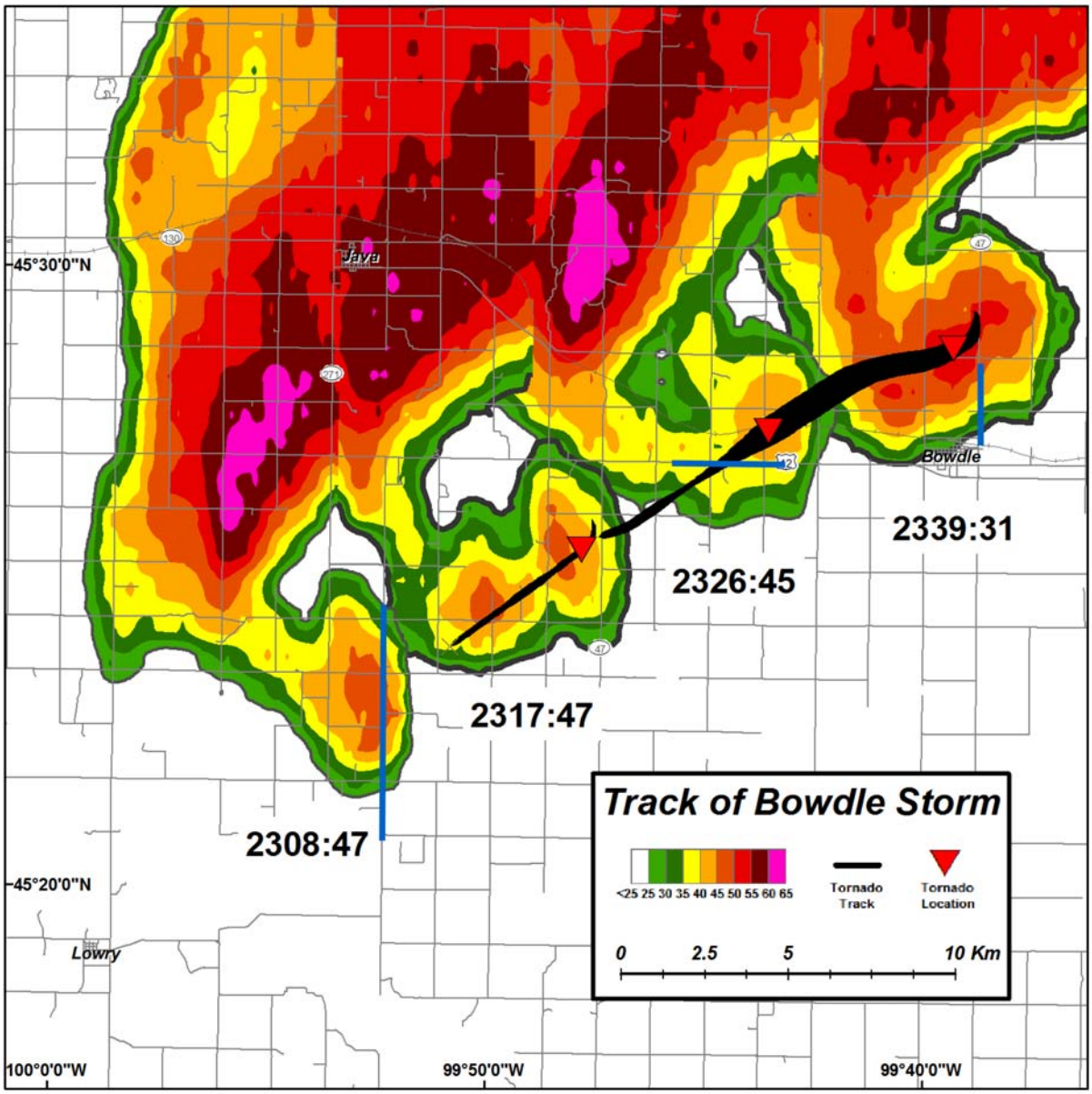

Fig. 1: Radar evolution from 2308:47 UTC – 2339:31 UTC and tornado tracks of the first two tornados produced by the Bowdle storm. Tornado positions at the radar times are indicated with red triangles. The mesonet sampling locations (ground relative) during cycles 2 and 3 are indicated by the blue lines.

3. MOBILE MESONET OBSERVATIONS

3.1 Cycle 1 (2230 UTC – 2245 UTC, non-tornadic)

Mesonet teams spread out along Highway 83 just south of the developing low-level mesocyclone at 2234 UTC and at 2337 UTC the RFD boundary passed over the mesonet. All teams saw negligible change from inflow conditions until ~ 2 minutes after the RFD boundary passage. The southernmost team (~ 2 miles south of the low level mesocyclone), experienced a 9 K θ_e drop and 1 K drop in θ_v from 2239 – 2240 UTC as the winds backed to a southwesterly direction. The northern teams then measured a ~4.5 K drop in θ_e, with little change in θ_v during the next minute. Tornadogenesis did not occur during this cycle despite the relatively "warm" RFD conditions over the mesonet north of the southernmost team. It should be noted that the wind speeds were relatively constant throughout the period at 10-15 kt (ground-relative) with a brief lull right at the boundary.

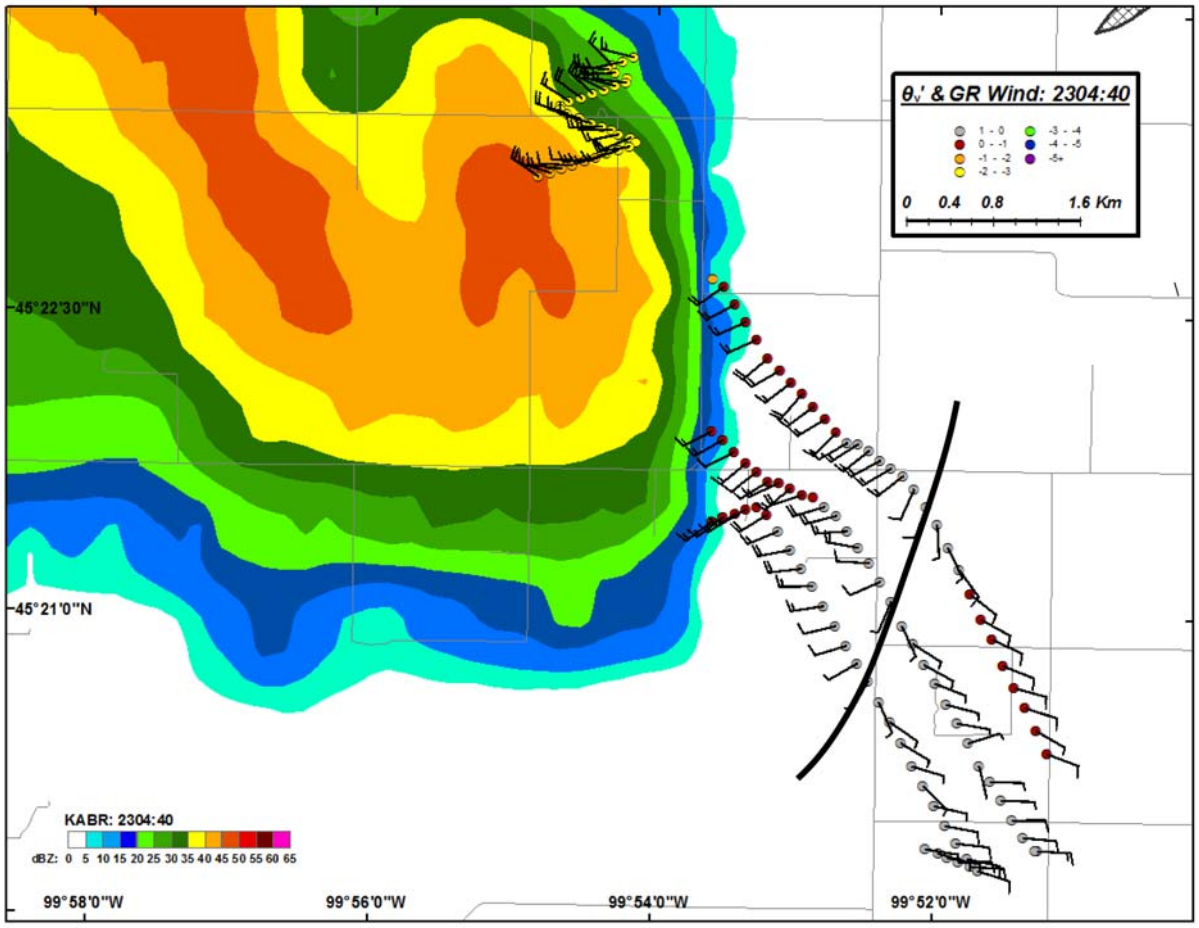

Fig. 2: Time-space conversion over a 5 minute period centered at 2304:40 UTC. Mesonet data are plotted every 10 s. The wind barbs depict the ground-relative wind in knots. The color on the mesonet positions shows the value of θ_v' in degrees Kelvin (scale in the upper right corner). The position of the initial RFDGF associated with the second mesocyclone cycle is indicated by the solid line.

3.2 Cycle 2 (2302 UTC – 2318 UTC, tornadic)

Teams followed the storm northeast and collected data in the RFD region as the storm reorganized and formed a new low-level mesocyclone ~ 8 miles northeast of Lowry as indicated in Fig. 1. Teams sampled the initial RFD with this cycle as they crossed the RFD boundary ~ 2304:40 UTC as shown in Fig. 2. The air immediately behind the RFDGF was similar in thermodynamic character to the inflow air, but θ_e values decreased by ~ 7K (θ_v decreased by ~ 2.5 K) over the next 5 minutes as the mesonet teams got further into the RFD.

By ~2309 UTC, the mesonet was arrayed on a N-S road that straddled a good portion of the tip of the hook echo on radar as shown in Fig. 3. At this time, the low-level mesocyclone was located between the 2 northern teams, and strong rotation was evident around the south side of the mesocyclone. Note that in the time period between ~ 2308 – 2310 UTC, all mesonet stations are stationary (or nearly stationary), but during this period, θ_e increased at the middle stations in the array, while θ_e decreased at the north and south stations. In an approximate 1 minute period surrounding the center time of the analysis, there is a significant θ_e gradient across the tip of the hook, with the largest θ_e deficits located along the north side of the low-level mesocyclone, and the area 2-3 km south of the mesocyclone where there is evidence of an anticyclonic flare in the wind field. During the same period, θ_v remains nearly constant (deficits of -2 to -2.5) across all measurement locations.

Between 2310:30 – 2311 UTC, an internal RFD surge passed through the mesonet. The RFD surge was marked by an increase in wind speed as the wind direction changed to NW, and a 0.5 - 1 K increase in both θ_e and θ_v at stations just south of the mesocyclone. A much larger increase in θ_e was measured at the southernmost station as shown in Fig. 4. Tornadogenesis of the first tornado produced

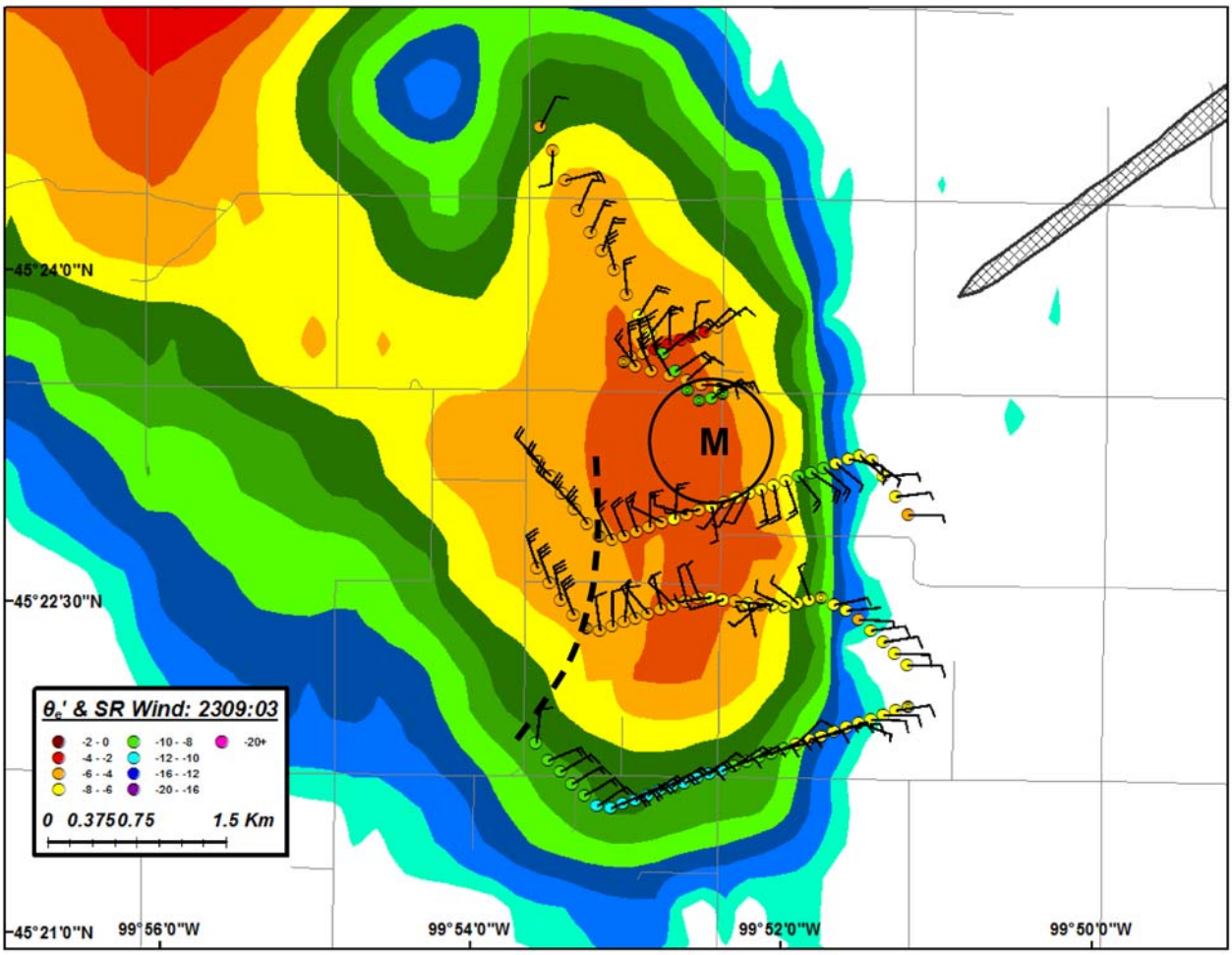

Fig. 3: Time-space conversion over a 5 minute period centered at 2309:03 UTC. Mesonet data are plotted every 10 s. The wind barbs depict the storm-relative wind in knots. The color on the mesonet positions shows the value of θ_e' in degrees Kelvin (scale in the lower left corner). The position of the low-level mesocyclone (circle) and an RFD surge boundary (dashed line) are indicated. The hatched region depicts the tornado track.

by this storm occurred approximately two minutes later at 2313 UTC 2 km east of the mesonet. Behind the RFD surge, θ_e and θ_v deficits remained relatively constant (~ -4.5 K and -2 K respectively) until the mesonet teams drove north into the northern portion of the hook echo.

3.3 Cycle 3 (2319 UTC – 2330 UTC, 2332 – 2345 UTC, tornadic)

The first tornado dissipated at 2318 UTC, and a second tornado quickly developed at ~23:19 UTC. This tornado ultimately developed into a large wedge tornado that produced EF-4 damage north of Bowdle. During the first ~5 minutes of the tornado's life, the vortex structure appeared to take on many forms from a single stout funnel to a large, diffuse multiple vortex circulation. The mesonet station responsible for in-situ probe deployment was positioned north of the developing tornado at 2319 UTC. Between ~2320 – 2327 UTC, the station collected measurements from sectors NNE through SW and within ~1-2 km of the developing tornado as shown in Fig. 5. CAPE values were extremely large (2500 – 4500 J kg^{-1}) surrounding the tornado in all measured quadrants, with values approaching those of the undisturbed storm inflow NE of the tornado. (Coincidently, this area lies along the tornado's path.) An internal RFD boundary can be inferred in the wind field to the southeast of the tornado at 2322:31 UTC, and CAPE values decrease to the south and west of this feature with the lowest CAPE values located SW of the tornado. Although the CAPE values were high through all sectors, θ_e deficits were notably larger than those typically seen in tornadic RFDs, with θ_e deficits of 8-10 K just south and southwest of the tornado.

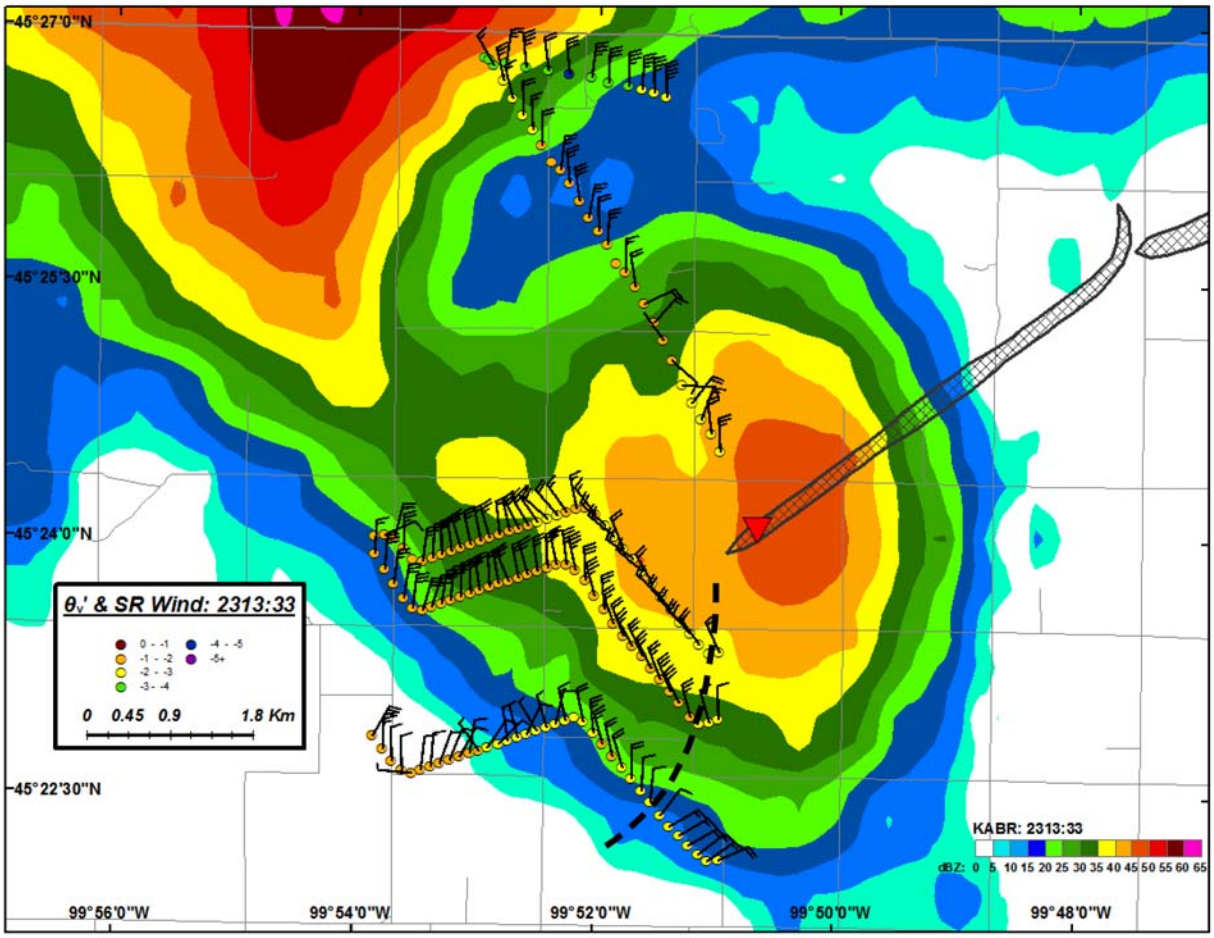

Fig. 4: Time-space conversion over a 6 minute period centered at 2313:33 UTC. Mesonet data are plotted every 10 s. The wind barbs depict the storm-relative wind in knots. The color on the mesonet positions shows the value of θ_v' in degrees Kelvin (scale in the lower left corner). The position of the RFD surge boundary (dashed line) and the position of the tornado in progress at the radar time (red triangle) are indicated. The hatched region depicts the tornado track.

After the tornado crossed Highway 12, the mesonet continued eastward and redeployed northeast of Bowdle as shown in Fig. 1. Teams crossed through an RFD boundary at ~ 2330 UTC during which storm-relative winds changed from WNW to ENE. The air mass east of the boundary was relative uniform with θ_e and θ_v deficits of ~6 K and 1 K respectively. It's likely that this boundary was an internal surge boundary as the values east of the boundary (particularly θ_e) didn't recover to environmental values and the ground-relative winds remained westerly.

At ~2336 UTC, the internal RFD boundary passes through the mesonet again, and θ_e (θ_v) began to slowly increase (decrease). Following the passage of this boundary, the wind field between the northern teams and the southern team become diffluent (and likely divergent) and it remained that way throughout the duration of this measurement period.

A strong RFD surge swept across the northern mesonet stations at ~3338 UTC as shown in Fig. 6. Although the southernmost station is only 1.5 km south of the northernmost station, it does not measure this surge until 3339:30 UTC. Behind the surge, both θ_e and θ_v increased, with θ_v deficits less than 1 K at most stations. Wind speeds also increased to 50-60 kts (ground relative). Within an ~1 minute period that coincided with the surge passing the mesonet, the tornado visually appeared to narrow (the shape changed from a wedge to more of a well-defined cylinder) and intensify. Note that the narrowing portion of the damage path is consistent with the tornado position at ~2338-2339 UTC, and this is also the approximate location of EF-4 damage to a farm site.

Approximately 4 minutes later at 2342 UTC, the final RFD surge passed through the mesonet. The thermodynamic characteristics of this surge were very

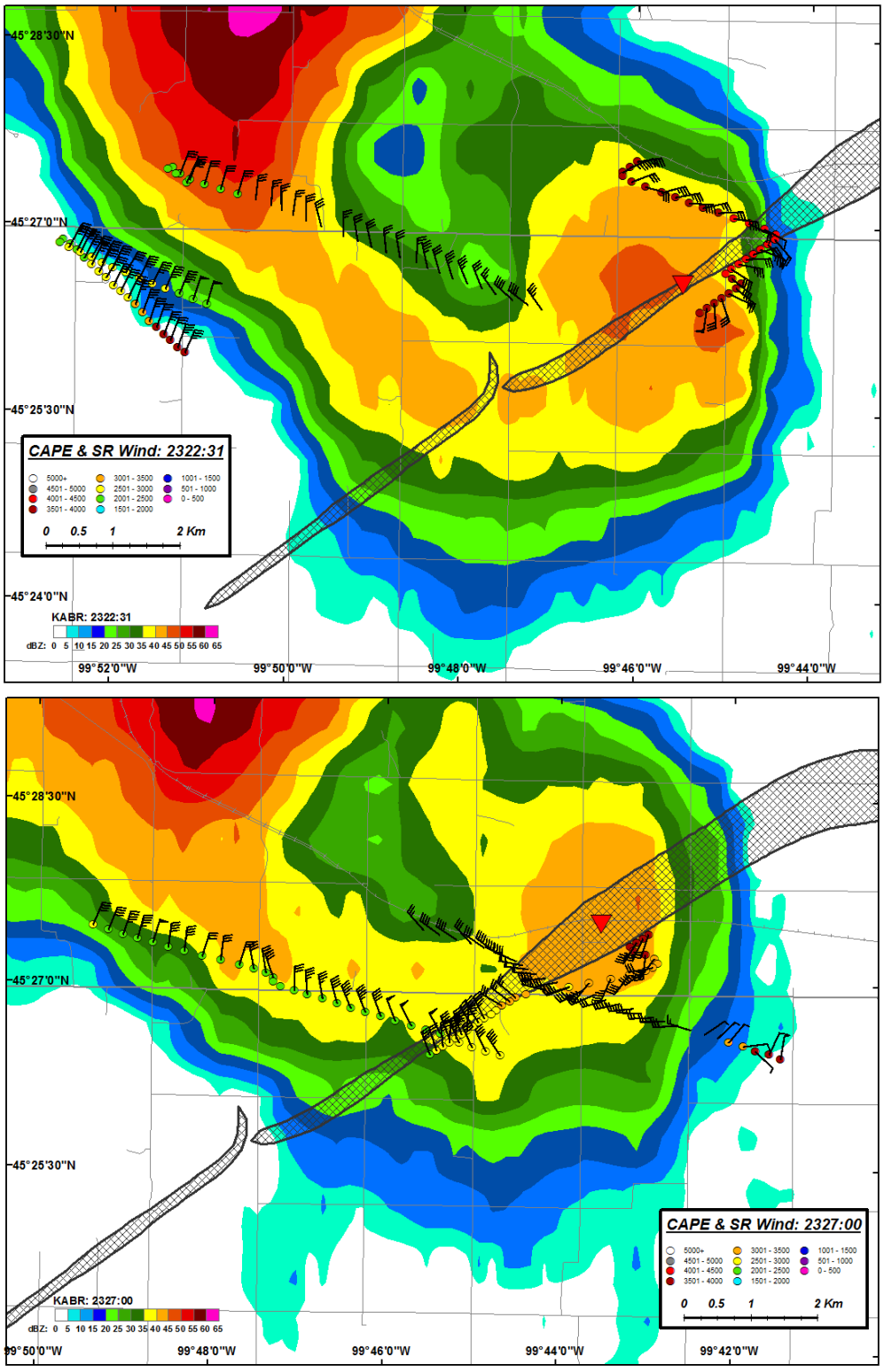

Fig. 5: Time-space conversion over a 5 minute period centered at 2322:31 UTC (top) and 2327 UTC (bottom). Mesonet data are plotted every 10 s. The wind barbs depict the storm-relative wind in knots. The color on the mesonet positions shows the value of Convective Available Potential Energy (CAPE) in $J(kg)^{-1}$ relative to the inflow sounding (scale shown in insets). The position of the tornado in progress at the radar time (red triangle) is indicated. The hatched region depicts the tornado track.

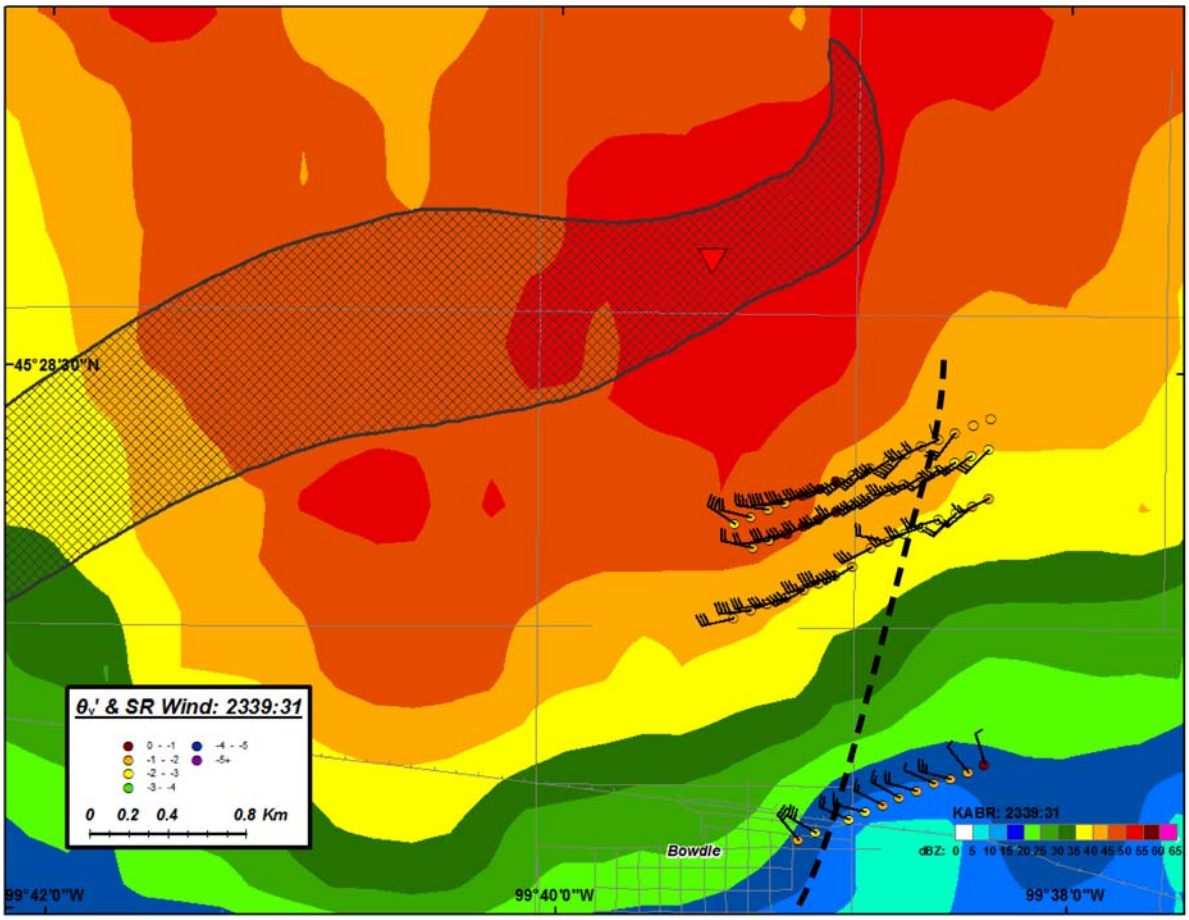

Fig. 6: Time-space conversion over a 5 minute period centered at 2339:31 UTC. Mesonet data are plotted every 20 s. The wind barbs depict the storm-relative wind in knots. The color on the mesonet positions shows the value of θ_v' in degrees Kelvin (scale in the lower left corner). The position of the RFD surge boundary (dashed line) and the position of the tornado in progress at the radar time (red triangle) are indicated. The hatched region depicts the tornado track.

different than previous surges as both θ_e and θ_v dropped rapidly behind the RFD surge boundary as shown in Fig. 7. By 2346 UTC, all stations were measuring θ_e deficits of 16-20 K and θ_v deficits of 5-6 K. During this time the tornado narrowed markedly and turned northward. At ~2344 UTC, moderate to heavy rain was falling at the northern mesonet stations and the tornado became obscured by rain. The estimated tornado dissipation time is ~2345 UTC based on the last known position and speed of the tornado and the location of the end of the damage path.

4. SUMMARY AND DISCUSSION

We have presented some preliminary analysis of the mobile mesonet data collected in the RFD region of a strong tornadic supercell near Bowdle, South Dakota on 22 May 2010. Four mesonet teams collected data in the RFD region of the storm through one nontornadic and two tornadic cycles.

Several internal RFD surges were sampled through multiple mesocyclone cycles. Two of the RFD surges were warmer (both in terms of θ_e and θ_v) than the air that preceded them and occurred in close proximity (time-wise) to tornadogenesis or apparent tornado intensification. This observation is consistent with warm RFD surges that have been measured in other cases (Finely and Lee 2004, 2008). One of the measured RFD surges was quite cold (both in term of θ_e and θ_v), and this surge closely preceded tornado dissipation. Although we are not aware of any reported cases of cold RFD surges prior to tornado dissipation, the trend of RFD air becoming colder in time toward the end of the tornado lifecycle has been noted previously (e.g., Lee et al. 2004; Hirth et al. 2008).

The RFD air to the south and southwest of the Bowdle tornado early in its life was relatively cool with respect to θ_e compared to the first tornadic RFD measured on this day and other typical tornadic RFDs (Markowski et al. 2002; Grzych et al. 2007). This air still possessed a significant amount of potential buoyancy however, given the large amount of CAPE in the environment. The tornado structure at this time appeared diffuse and

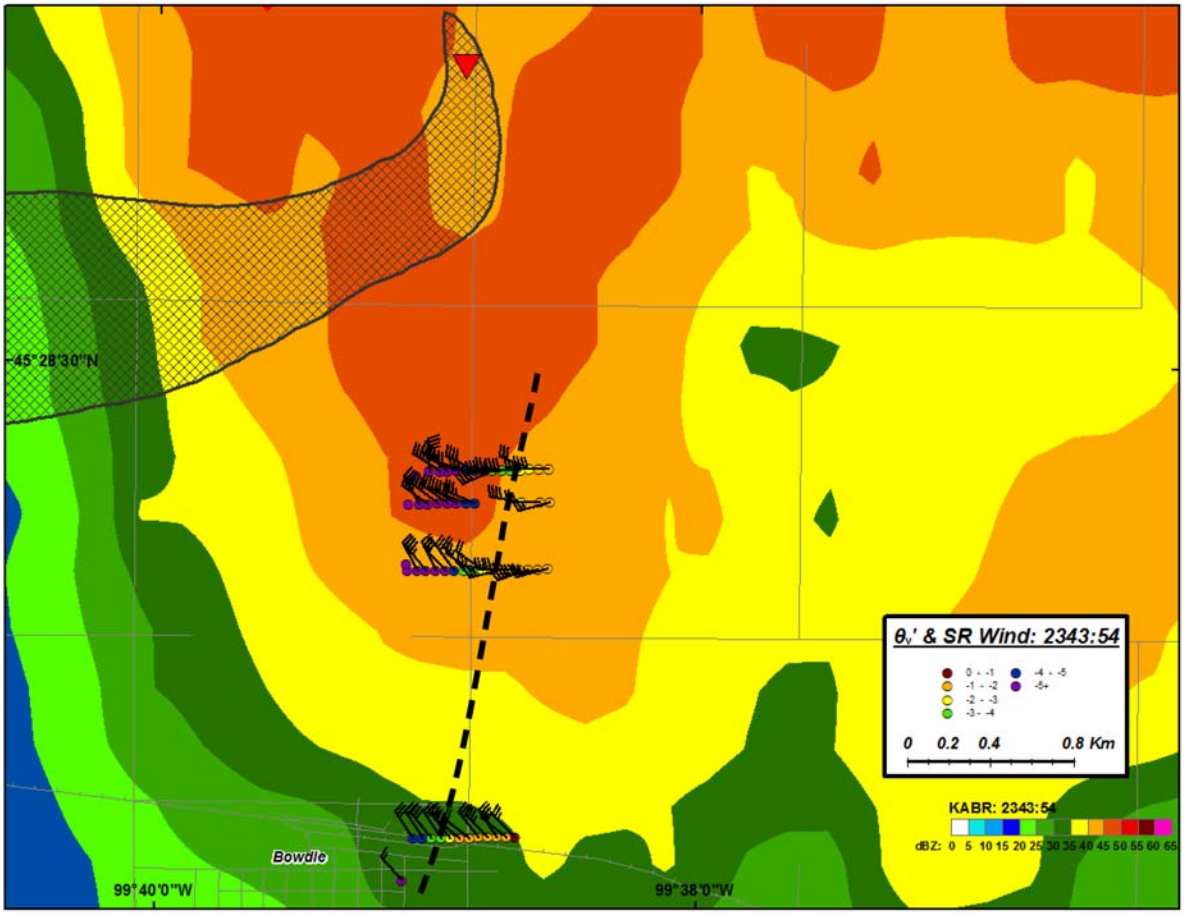

Fig. 7: Time-space conversion over a 5 minute period centered at 2343:54 UTC. Mesonet data are plotted every 20 s. The wind barbs depict the storm-relative wind in knots. The color on the mesonet positions shows the value of θ_v' in degrees Kelvin (scale in the lower left corner). The position of the RFD surge boundary (dashed line) and the position of the tornado in progress at the radar time (red triangle) are indicated. The hatched region depicts the tornado track.

somewhat disorganized compared to later in its lifecycle when the RFD air was significantly warmer.

One nontornadic RFD was sampled early in the storm's life. Both θ_e and θ_v were quite warm during the measurement period, but the kinematic fields were relatively weak compared to other RFDs measured on this day. Additional analysis of the dataset is underway to better understand the nature and source regions for air in the RFD surges.

5. ACKNOWLEDGEMENTS

All participants of TWISTEX are thanked for their contributions to the data collection during the project. Jon Merage and Sean Mullins are thanked for generously providing additional mesonet data. Partial support for author Karstens was provided by NOAA grants NA06OAR4600230, NA08OAR4600887, and NA09OAR4600222.

6. REFERENCES

Finley, C.A. and B.D Lee, 2008: Mobile Mesonet Observations of an Intense RFD and Multiple RFD Gust Fronts in the May 23 Quinter, Kansas Tornadic Supercell during TWISTEX 2008. *Electronic Proceedings, 24th Conference on Severe Local Storms,* Savannah, GA, Amer. Meteor. Soc.

Finley, C.A., and B.D. Lee, 2004: High Resolution Mobile Mesonet Observations of RFD Surges in the June 9 Basset, Nebraska Supercell During Project Answers 2003. *Electronic Proceedings, 22nd Conference on Severe Local Storms,* Hyannis, MA, Amer. Meteor. Soc., 531-534.

Grzych, M. L., B. D. Lee, and C. A. Finley, 2007: Thermodynamic analysis of supercell rear-flank downdrafts from Project ANSWERS 2003. *Mon. Wea. Rev.*, **35**, 240-246.

Hirth, B., J. L. Schroeder and C. C. Weiss, 2008: Surface Analysis of the Rear-Flank Downdraft Outflow in Two Tornadic Supercells. *Mon. Wea. Rev.* **136**, 2344-2363.

Lee, B.D., C.A. Finley and P. Skinner, 2004: Thermodynamic and Kinematic Analysis of Multiple RFD Surges for the 24 June 2003 Manchester, South Dakota Cyclic Tornadic Supercell During Project ANSWERS 2003. *Electronic Proceedings, 22nd Conference on Severe Local Storms,* Hyannis, MA, Amer. Meteor. Soc.

Markowski, P. M., J. M. Straka, and E. N. Rasmussen, 2002: Direct surface thermodynamic observations within rear-flank downdrafts of non-tornadic and tornadic supercells. *Mon. Wea. Rev.* **130**, 1692-1721.

Straka, J. M., E. N. Rasmussen, and S. E. Fredrickson, 1996: A mobile mesonet for fine-scale meteorological observations. *J. Atmos. Oceanic Technol.*, **13**, 921-936.